Relativistic many-body calculations of excitation energies and oscillator strengths in Ni-like ions

U. I. Safronova and W. R. Johnson
Department of Physics, University of Notre Dame, Notre Dame, Indiana 46556

J. R. Albritton
Lawrence Livermore National Laboratory, P.O. Box 808, Livermore, California 94551

(Received 8 May 2000; published 11 October 2000)

Excitation energies for $3l$-$4l'$ particle-hole states of Ni-like ions are determined to second order in relativistic many body perturbation theory. The calculations start from a closed-shell Dirac-Fock potential, and include second-order Coulomb and Breit-Coulomb interactions. Retarded electric-dipole matrix elements (in length and velocity forms) are calculated in second order for transitions from excited $3l$-$4l'$ states to the closed-shell ground state. Wavelengths for 3-4 and 4-4 transitions are compared with experimental data, and with other high-precision calculations. Trends of oscillator strengths as functions of nuclear charge Z are shown graphically for selected transitions.

PACS number(s): 32.30.Rj, 32.70.Cs, 31.25.Jf, 31.15.Md

I. INTRODUCTION

This is the second in a series of relativistic many-body perturbation theory (MBPT) studies of atomic characteristics of particle-hole excitations of closed-shell ions. In the first of these studies, energies [1–3] and oscillator strengths [4] in Ne-like ions were considered by Avgoustoglou and co-workers.

The second-order MBPT calculations for Ni-like ions start from a $1s^22s^22p^63s^23p^63d^{10}$ Dirac-Fock potential. We consider all possible $3l$ holes and $4l$ particles leading to 56 odd-parity and 50 even-parity $3l^{-1}4l'(J)$ states. We calculate energies of the 106 states for 18 representative ions with nuclear charge Z ranging from 47 to 82. For odd-parity states with $J=1$, we extend our calculations of energies to Z from 47 to 92, and line strengths to Z from 32 to 100.

The Ni-isoelectronic sequence has been studied extensively, especially in recent years, in connection with x-ray lasers. The lasing action occurs because the $3d^{-1}4d$ levels are metastable to radiative decay to the Ni-like ground state; the transitions to the ground state from the lower $3d^{-1}4p$ levels are of course radiatively allowed. Ni-like x-ray lasers were first demonstrated in 1987 in a laser produced plasma of Eu, and later in laser-produced plasmas of Ta, W, and Au (see Refs. [5,6], and references therein). Accurate knowledge of the lasing wavelengths is essential for applications to laboratory x-ray lasers. Wavelength of $3d^94d\,^1S_0$-$3d^94p\,^1P_1$ x-ray lines in several low-Z Ni-like ions ranging from Y ($Z=39$) to Cd ($Z=48$) were measured recently by Li *et al.* [7]. Measurements for two lasing lines: $3d_{3/2}4d_{3/2}(0)$-$3d_{5/2}4p_{3/2}(1)$ and $3d_{3/2}4d_{3/2}(0)$-$3d_{5/2}4p_{1/2}(1)$ in ions ranging from Nd ($Z=60$) to Ta ($Z=73$) were reported by Daido *et al.* in Ref. [8]. It should be noted that neither LS- nor jj-coupling schemes described these states properly; this is why different designations are used for these states in Refs. [7] and [8]. Lasing on the Ni-like $3d^94f\,^1P_1$–$3d^94d\,^1P_1$ x-ray line in Zr ($Z=40$), Nb ($Z=41$), and Mo ($Z=42$) was reported recently by Nilsen *et al.* in Ref. [9]. Measured wavelengths were presented for these ions as well as predicted values for ions from $Z=36$ to 54. The predictions in Ref. [9] were made by fiting the differences between energies calculated with the multiconfiguration Dirac-Fock (MCDF) code, and experimentally determined energies for $Z=37$–42 to a straight line. A similar method was used for predicting lasing lines in Refs. [5] and [7]. Accurate theoretical values for two lasing lines: $3d_{3/2}4d_{3/2}(0)$-$3d_{5/2}4p_{3/2}(1)$ and $3d_{3/2}4d_{3/2}(0)$-$3d_{5/2}4p_{1/2}(1)$ in selected Ni-like ions with Z from 60 to 73 were presented in Ref. [8], where it was shown that good agreement between theoretical and experimental wavelengths could be obtained by taking into account the d-correlation.

A detailed analysis of 3-4 transitions in the x-ray spectrum by laser produced plasmas of Ba ($Z=56$), La ($Z=57$), and Pr ($Z=59$) was reported recently by Doron *et al.* [10] and Zigler *et al.* [11]. Ab-initio calculations were performed in Ref. [10] using the RELAC relativistic computer code to identify $3d$-nf $(n=4-8)$, $3p$-$4s$, and $3p$-$4d$ transitions of Ni-like Ba. The same computer code was used by Busquet *et al.* [12] to identify x-ray spectral lines emitted by a target of Au ($Z=79$). In Ref. [12], a detailed description of the RELAC code, which is based on a relativistic model potential, was given. The HULLAC package is also based on a relativistic model potential [13]. The $n=3$–4 transitions observed in x-ray spectra of Ni-like ions (Ag^{19+}-Pb^{54+}) were investigated theoretically by Quinet and Biémont [14], where the MCDF approach (Grant's code) was used to calculate wavelengths and oscillator strengths for the $3d$-$4p$, $3d$-$4f$, $3p$-$4s$, and $3p$-$4d$ electric-dipole transitions. The theoretical results in Ref. [14] were compared with all previous published experimental data obtained from x-ray spectra emitted by strongly ionized atoms, and generated by vacuum sparks, Tokamaks or high power lasers and the difference between theoretical and experimental values for the 3-4 transition were found to be about 0.5%.

There are fewer papers concerned with the analysis of the $4s$-$4p$ and $4p$-$4d$ transitions in Ni-like ions. Spectra of 4-4 transitions in a laser-produced plasma of Ni-like ions

1050-2947/2000/62(5)/052505(14)/$15.00

(Ru^{16+}-Sn^{22+}) were observed and analyzed by Churilov *et al.* in Ref. [15]. The analysis of these spectra was based on the theoretical prediction by Wyart [16]. The prediction of $4s$-$4p$ and $4p$-$4d$ transitions in Ni-like ions (Mo^{14+}-Sn^{22+}) in Ref. [16] was based on Slater-Condon-type calculations of $3d^9 4s$, $3d^9 4p$, and $3d^9 4d$ configurations. The radial parameters involved in the three configurations were determined by a generalized least-squares fit using all known levels in the sequence.

In the present paper, a relativistic MBPT is used to determine energies of $3l^{-1}4l'(J)$ states of Ni-like ions. Energies are calculated for the 56 odd-parity $3d^{-1}4p(J)$, $3d^{-1}4f(J)$, $3p^{-1}4s(J)$, $3p^{-1}4d(J)$, $3s^{-1}4p(J)$, and $3s^{-1}4f(J)$ excited states and the 50 even-parity $3d^{-1}4s(J)$, $3d^{-1}4d(J)$, $3p^{-1}4p(J)$, $3p^{-1}4f(J)$, $3s^{-1}4s(J)$, and $3s^{-1}4d(J)$ excited states for 18 representative Ni-like ions with $Z=47$–82. The energies of the 13 odd-parity states with $J=1$ are calculated for Ni-like ions with $Z=47$–92.

Relativistic MBPT is also used to determine reduced matrix elements and oscillator strengths for electric dipole transitions from the $3l^{-1}4l'(1)$ states to the ${}^1S_0$ ground state in Ni-like ions with nuclear charges Z ranging from 32 to 100. Retarded $E1$ matrix elements are evaluated in both length and velocity forms. The MBPT calculations start from a nonlocal $1s^2 2s^2 2p^6 3s^2 3p^6 3d^{10}$ Dirac-Fock potential, and consequently give gauge-dependent transition matrix elements. Second-order correlation corrections compensate almost exactly for the gauge dependence of the first-order matrix elements, leading to corrected matrix elements that differ by less than 1% in length and velocity forms throughout the periodic system.

II. METHOD

Details of the MBPT method were presented in Ref. [1] for a calculation of energies of particle-hole states, in Ref. [17] for calculation of energies of particle-particle states, and in Ref. [18] for calculation of radiative transition rates in two-particle states. Here we will present only the model space for Ni-like ions and the first- and second-order diagram contributions for particle-hole systems without repeating the detailed discussions given in Refs. [1], [17], and [18].

A. Model space

For atoms with one hole in closed shells and one electron above closed shells, the model space is formed from particle-hole states of the type $a_v^+ a_a|0\rangle$, where $|0\rangle$ is the closed-shell $1s_{1/2}^2 2s_{1/2}^2 2p_{1/2}^2 2p_{3/2}^4 3s_{1/2}^2 3p_{1/2}^2 3p_{3/2}^4 3d_{3/2}^4 3d_{5/2}^6$ ground state. The single-particle indices v range over states in the valence shell and the single-hole indices a range over the closed core. For our study of low-lying states $3l^{-1}4l'$ states of Ni-like ions, values of a are $3s_{1/2}$, $3p_{1/2}$, $3p_{3/2}$, $3d_{3/2}$, and $3d_{5/2}$, while values of v are $4s_{1/2}$, $4p_{1/2}$, $4p_{3/2}$, $4d_{3/2}$, $4d_{5/2}$, $4f_{5/2}$, and $4f_{7/2}$. To obtain orthonormal model states, we consider the coupled states $\Phi_{JM}(av)$ defined by

$$\Phi_{JM}(av)=\sqrt{(2J+1)}\sum_{m_a m_v}(-1)^{j_v-m_v}\times\begin{pmatrix} j_v & J & j_a \\ -m_v & M & m_a\end{pmatrix} a^\dagger_{v m_v} a_{a m_a}|0\rangle. \quad (2.1)$$

Combining the $n=3$ hole orbitals and the $n=4$ particle orbitals in nickel, we obtain 56 odd-parity states consisting of five $J=0$ states, 13 $J=1$ states, 15 $J=2$ states, 12 $J=3$ states, seven $J=4$ states, two $J=5$ states, and two $J=6$ states. Additionally, there are 50 even-parity states consisting of five $J=0$ states, 12 $J=1$ states, 14 $J=2$ states, 11 $J=3$ states, six $J=4$ states, one $J=5$ state, and one $J=6$ state. The distribution of the 116 states in the model space is summarized in Table I.

B. Energy matrix

The first-order energy-matrix element for a particle-hole system $va(J)$ is

$$E^{(1)}[a'v'(J),av(J)]=\delta_{vv'}\delta_{aa'}(\epsilon_v-\epsilon_a)+\frac{1}{(2J+1)}\times(-1)^{j_v+j_a+J+1}Z_J(av'va'), \quad (2.2)$$

where ϵ_i is the eigenvalue of the Dirac-Hartree-Fock (DHF) equation for state i, and where

$$Z_J(abcd)=X_J(abcd)+\sum_k (2J+1)X_k(abdc)\times\begin{Bmatrix} j_a & j_c & J \\ j_b & j_d & k\end{Bmatrix}, \quad (2.3)$$

with

$$X_k(abcd)=\langle a||C_k||c\rangle\langle b||C_k||d\rangle R_k(abcd). \quad (2.4)$$

The quantities C_k are normalized spherical harmonics and $R_k(abcd)$ are Slater integrals. The corresponding second-order energy matrix is

$$E^{(2)}[a'v'(J),av(J)]=\delta_{vv'}\delta_{aa'}(E_v^{(2)}+E_a^{(2)})+\sum_{i=1,4}E^{R_i}[a'v'(J),av(J)]. \quad (2.5)$$

The second-order one-particle $E_v^{(2)}$ and one-hole $E_a^{(2)}$ contributions are defined by three terms: double sums, single sums, and a one-potential term. This later term contributes only to the Breit-Coulomb correction. The second-order contribution for hole state a ($E_a^{(2)}$) is

TABLE I. Possible hole-particle states in the $3lj4l'j'$ complex; jj-coupling scheme.

Odd-parity states				
$J=0$	$J=1$	$J=2$	$J=3$	$J=4$-6
$3d_{3/2}4p_{3/2}(0)$	$3d_{5/2}4p_{3/2}(1)$	$3d_{5/2}4p_{1/2}(2)$	$3d_{5/2}4p_{1/2}(3)$	$3d_{5/2}4p_{3/2}(4)$
$3d_{5/2}4f_{5/2}(0)$	$3d_{3/2}4p_{1/2}(1)$	$3d_{5/2}4p_{3/2}(2)$	$3d_{5/2}4p_{3/2}(3)$	$3d_{5/2}4f_{5/2}(4)$
$3p_{1/2}4s_{1/2}(0)$	$3d_{3/2}4p_{3/2}(1)$	$3d_{3/2}4p_{1/2}(2)$	$3d_{3/2}4p_{3/2}(3)$	$3d_{5/2}4f_{7/2}(4)$
$3p_{3/2}4d_{3/2}(0)$	$3d_{5/2}4f_{5/2}(1)$	$3d_{3/2}4p_{3/2}(2)$	$3d_{5/2}4f_{5/2}(3)$	$3d_{3/2}4f_{5/2}(4)$
$3s_{1/2}4p_{1/2}(0)$	$3d_{5/2}4f_{7/2}(1)$	$3d_{5/2}4f_{5/2}(2)$	$3d_{5/2}4f_{7/2}(3)$	$3d_{3/2}4f_{7/2}(4)$
	$3d_{3/2}4f_{5/2}(1)$	$3d_{5/2}4f_{7/2}(2)$	$3d_{3/2}4f_{5/2}(3)$	$3p_{3/2}4d_{5/2}(4)$
	$3p_{3/2}4s_{1/2}(1)$	$3d_{3/2}4f_{5/2}(2)$	$3d_{3/2}4f_{7/2}(3)$	$3s_{1/2}4f_{7/2}(4)$
	$3p_{1/2}4s_{1/2}(1)$	$3d_{3/2}4f_{7/2}(2)$	$3p_{3/2}4d_{3/2}(3)$	$3d_{5/2}4f_{5/2}(5)$
	$3p_{3/2}4d_{3/2}(1)$	$3p_{3/2}4s_{1/2}(2)$	$3p_{3/2}4d_{5/2}(3)$	$3d_{5/2}4f_{7/2}(5)$
	$3p_{3/2}4d_{5/2}(1)$	$3p_{3/2}4d_{3/2}(2)$	$3p_{1/2}4d_{5/2}(3)$	$3d_{3/2}4f_{7/2}(5)$
	$3p_{1/2}4d_{3/2}(1)$	$3p_{3/2}4d_{5/2}(2)$	$3s_{1/2}4f_{5/2}(3)$	$3d_{5/2}4f_{7/2}(6)$
	$3s_{1/2}4p_{1/2}(1)$	$3p_{1/2}4d_{3/2}(2)$	$3s_{1/2}4f_{7/2}(3)$	
	$3s_{1/2}4p_{3/2}(1)$	$3p_{1/2}4d_{5/2}(2)$		
		$3s_{1/2}4p_{3/2}(2)$		
		$3s_{1/2}4f_{5/2}(2)$		
Even-parity states				
$J=0$	$J=1$	$J=2$	$J=3$	$J=4$-5
$3d_{5/2}4d_{5/2}(0)$	$3d_{3/2}4s_{1/2}(1)$	$3d_{5/2}4s_{1/2}(2)$	$3d_{5/2}4s_{1/2}(3)$	$3d_{5/2}4d_{3/2}(4)$
$3d_{3/2}4d_{3/2}(0)$	$3d_{5/2}4d_{3/2}(1)$	$3d_{3/2}4s_{1/2}(2)$	$3d_{5/2}4d_{3/2}(3)$	$3d_{5/2}4d_{5/2}(4)$
$3p_{3/2}4p_{3/2}(0)$	$3d_{5/2}4d_{5/2}(1)$	$3d_{5/2}4d_{3/2}(2)$	$3d_{5/2}4d_{5/2}(3)$	$3d_{3/2}4d_{5/2}(4)$
$3p_{1/2}4p_{1/2}(0)$	$3d_{3/2}4d_{3/2}(1)$	$3d_{5/2}4d_{5/2}(2)$	$3d_{3/2}4d_{3/2}(3)$	$3p_{3/2}4f_{5/2}(4)$
$3s_{1/2}4s_{1/2}(0)$	$3d_{3/2}4d_{5/2}(1)$	$3d_{3/2}4d_{3/2}(2)$	$3d_{3/2}4d_{5/2}(3)$	$3p_{3/2}4f_{7/2}(4)$
	$3p_{3/2}4p_{1/2}(1)$	$3d_{3/2}4d_{5/2}(2)$	$3p_{3/2}4p_{3/2}(3)$	$3p_{1/2}4f_{7/2}(4)$
	$3p_{3/2}4p_{3/2}(1)$	$3p_{3/2}4p_{1/2}(2)$	$3p_{3/2}4f_{5/2}(3)$	$3d_{5/2}4d_{5/2}(5)$
	$3p_{1/2}4p_{1/2}(1)$	$3p_{3/2}4p_{3/2}(2)$	$3p_{1/2}4f_{5/2}(3)$	$3p_{3/2}4f_{7/2}(5)$
	$3p_{1/2}4p_{3/2}(1)$	$3p_{1/2}4p_{3/2}(2)$	$3p_{3/2}4f_{7/2}(3)$	
	$3p_{3/2}4f_{5/2}(1)$	$3p_{3/2}4f_{5/2}(2)$	$3p_{1/2}4f_{7/2}(3)$	
	$3s_{1/2}4s_{1/2}(1)$	$3p_{3/2}4f_{7/2}(2)$	$3s_{1/2}4d_{5/2}(3)$	
	$3s_{1/2}4d_{3/2}(1)$	$3p_{1/2}4f_{5/2}(2)$		
		$3s_{1/2}4d_{3/2}(2)$		
		$3s_{1/2}4d_{5/2}(2)$		

$$E_a^{(2)}=-\sum_{cmn}\sum_k\frac{(-1)^{j_m+j_n-j_a-j_c}}{(2j_a+1)(2k+1)}\frac{X_k(acmn)Z_k(mnac)}{\epsilon_{ac}-\epsilon_{mn}}+\sum_{bcn}\sum_k\frac{(-1)^{j_a+j_n-j_b-j_c}}{(2j_a+1)(2k+1)}\frac{Z_k(bcan)X_k(anbc)}{\epsilon_{bc}-\epsilon_{an}}$$
$$-2\sum_{nb}\delta_{j_bj_n}\sqrt{\frac{2j_b+1}{2j_a+1}}\frac{\Delta(bn)Z_0(naba)}{\epsilon_b-\epsilon_n}, \tag{2.6}$$

where

$$\Delta(bn)=\sum_c\delta_{j_bj_n}\sqrt{\frac{2j_c+1}{2j_b+1}}Z_0(bcnc). \tag{2.7}$$

Labels b and c designate core states, and m and n designate virtual states. The second-order energy for the valence electron v ($E_v^{(2)}$) is found by replacing a by v in the above expression and changing the sign of each term. The second-order particle-hole interaction energies $E^{R_i}([a'v'(J),av(J)]$ are

$$E^{R_1}[a'v'(J),av(J)]=\sum_{mn}\sum_{kk'}(-1)^{J+j_a-j_v}\begin{Bmatrix}k & k' & J\\ j_a & j_v & j_m\end{Bmatrix}\begin{Bmatrix}k & k' & J\\ j_{v'} & j_{a'} & j_n\end{Bmatrix}\frac{X_k(va'mn)Z_{k'}(nmv'a)}{\varepsilon_{va'}-\varepsilon_{nm}}, \tag{2.8}$$

$$E^{R_2}[a'v'(J),av(J)]=\sum_{bc}\sum_{kk'}(-1)^{J+j_a-j_v}\begin{Bmatrix} k & k' & J \\ j_v & j_a & j_b \end{Bmatrix}\begin{Bmatrix} k & k' & J \\ j_{a'} & j_{v'} & j_c \end{Bmatrix}\frac{X_k(bcav')Z_{k'}(a'vcb)}{\varepsilon_{bc}-\varepsilon_{v'a}}, \tag{2.9}$$

$$E^{R_3}[a'v'(J),av(J)]=\frac{1}{(2J+1)^2}\sum_{nb}(-1)^{j_{a'}+j_b-j_{v'}-j_n}\left[\frac{Z_J(a'bv'n)Z_J(vnab)}{\varepsilon_{ba'}-\varepsilon_{v'n}}+\frac{Z_J(vban)Z_J(a'nv'b)}{\varepsilon_{vb}-\varepsilon_{na}}\right]$$
$$+\sum_{nb}\sum_{k}\frac{1}{2k+1}(-1)^{j_{v'}+j_{a'}+j_b+j_n+k+J}\begin{Bmatrix} j_v & j_a & J \\ j_{a'} & j_{v'} & k \end{Bmatrix}\left[\frac{Z_k(vbv'n)Z_k(a'nab)}{\varepsilon_{bv}-\varepsilon_{v'n}}\right.$$
$$\left.+\frac{Z_k(a'ban)Z_k(vnv'b)}{\varepsilon_{a'b}-\varepsilon_{na}}\right] \tag{2.10}$$

$$E^{R_4}(a'v'J,avJ)=\frac{1}{(2J+1)}(-1)^{j_{v'}-j_{a'}+J}\left[\sum_{n\neq v}\delta(j_vj_n)\frac{\Delta(vn)Z_J(na'av')}{\varepsilon_v-\varepsilon_n}+\sum_n\delta(j_{a'}j_n)\frac{\Delta(a'n)Z_J(vnav')}{\varepsilon_{a'}-\varepsilon_n}\right.$$
$$+\sum_c\delta(j_{v'}j_c)\frac{Z_J(va'ac)\Delta(cv')}{\varepsilon_{v'}-\varepsilon_c}+\sum_{c\neq a}\delta(j_aj_c)\frac{Z_J(va'cv')\Delta(ca)}{\varepsilon_a-\varepsilon_c}+\sum_n\delta(j_aj_n)\frac{Z_J(va'nv')\Delta(na)}{\varepsilon_{va'}-\varepsilon_{nv'}}$$
$$+\sum_{n(na\neq va')}\delta(j_{v'}j_n)\frac{Z_J(va'an)\Delta(nv')}{\varepsilon_{va'}-\varepsilon_{na}}+\sum_{c(cv\neq v'a)}\delta(j_{a'}j_c)\frac{\Delta(a'c)Z_J(vcav')}{\varepsilon_{v'a}-\varepsilon_{cv}}$$
$$\left.+\sum_c\delta(j_vj_c)\frac{\Delta(vc)Z_J(ca'av')}{\varepsilon_{v'a}-\varepsilon_{ca'}}\right]. \tag{2.11}$$

All of the above expressions were defined for the Coulomb interaction. When we include the Breit interaction in the calculation, the Coulomb matrix element $X_k(ab,cd)$ is modified according to the rule

$$X_k(ab,cd)\Rightarrow X_k(ab,cd)+M_k(ab,cd)+N_k(ab,cd). \tag{2.12}$$

The magnetic radial integrals M and N are defined by Eqs. (A4) and (A5) in Ref. [19].

C. Example: Energy matrix for Ba^{28+}

In Tables II and III, we give details of the second-order energies for the special case of Ni-like barium, $Z=56$. The headings used in these tables are the same as those used in Ref. [17]. In Table II, we show the second-order contributions to the valence $E_v^{(2)}$ and hole $E_a^{(2)}$ energies, defined in Eq. (2.6). Contributions from each of the three distinct terms—double sum V_1, single sum V_2, and one-potential term V_3—are given in this table. In the upper panels, second-order Coulomb contributions are presented for $n=3$ hole states and $n=4$ particle states and, in the lower panel, second-order Breit-Coulomb corrections are listed. The single sum contribution to hole states dominates the Coulomb corrections shown in the upper panel. The one-potential term V_3 contributes only to the Coulomb-Breit correction; where it is the dominant contribution. In Table III we give diagonal matrix elements of the second-order interaction energy for the particle-hole system defined in Eqs. (2.8)–(2.11) for odd-parity states with $J=1$. Coulomb contributions are given in the upper panels, and the Breit-Coulomb corrections are given in the lower ones. The largest contribution is from the term R_3 for the Coulomb interaction and from the term R_4 for the second-order Breit correction.

The orbitals used in the present calculation were obtained as linear combinations of B splines. These B-spline basis orbitals were determined using the method described in Ref. [20]. We used 40 B splines of order 8 for each single-particle angular momentum state, and we included all orbitals with orbital angular momentum $l\leqslant 7$ in our single-particle basis.

In Sec. II B, we gave analytical formulas for the first- and second-order contributions $E^{(1)}[a'v'(J),av(J)]$, $E^{(2)}[a'v'(J),av(J)]$, and $B^{(2)}[a'v'(J),av(J)]$ to the energy matrix. To determine the first-order energies of the states under consideration, we diagonalize the symmetric first-order effective Hamiltonian, including both the Coulomb and Breit interactions. The first-order expansion coefficient $C_1^N[av(J)]$ is the Nth eigenvector of the first-order effective Hamiltonian, and $E^{(1)}[N]$ is the corresponding eigenvalue. The resulting eigenvectors are used to determine the second-order Coulomb correction $E^{(2)}[N]$, the second-order Breit correction $B^{(2)}[N]$, and the QED correction $E_{\mathrm{Lamb}}[N]$. Usually, either LS or jj designations are used to label the resulting eigenvectors rather than simply enunerating with an index N. Here we use jj designations, since they are more suitable in Ni-like ions.

In Table IV, we list the following contributions to the energies of odd-parity $J=1$ states in Ba^{28+}: $E^{(0+1)}=E^{(0)}$

TABLE II. Contributions to the one-electron $E_v^{(2)}$ and one-hole energy $E_a^{(2)}$ for ions with a $1s^2 2s^2 2p^6 3s^2 3p^6 3d^{10}$ core from the three diagrams V_1–V_3 evaluated for the case of barium, $Z=56$.

	(a) Coulomb interaction:			
	V_1^{HF}	V_2^{HF}	V_3^{HF}	Σ^{HF}
$3s_{1/2}$	0.078365	-0.312162		-0.233798
$3p_{1/2}$	0.096743	-0.308099		-0.211356
$3p_{3/2}$	0.094550	-0.278281		-0.183730
$3d_{3/2}$	0.147751	-0.250838		-0.103087
$3d_{5/2}$	0.146695	-0.242938		-0.096243
$4s_{1/2}$	-0.080184	0.017005		-0.063179
$4p_{1/2}$	-0.082620	0.017788		-0.064831
$4p_{3/2}$	-0.076963	0.017584		-0.059379
$4d_{3/2}$	-0.081181	0.017376		-0.063805
$4d_{5/2}$	-0.078257	0.017296		-0.060960
$4f_{5/2}$	-0.067856	0.012001		-0.055855
$4f_{7/2}$	-0.066848	0.012194		-0.054655
	(b) Breit correction:			
	V_1^{BHF}	V_2^{BHF}	V_3^{BHF}	Σ^{BHF}
$3s_{1/2}$	0.002252	-0.001469	0.032447	0.033230
$3p_{1/2}$	0.003539	-0.001733	0.034512	0.036319
$3p_{3/2}$	0.003093	-0.001512	0.033207	0.034788
$3d_{3/2}$	0.003933	-0.002244	0.037250	0.038939
$3d_{5/2}$	0.003370	-0.001463	0.036691	0.038598
$4s_{1/2}$	-0.000596	0.000166	-0.007427	-0.007856
$4p_{1/2}$	-0.000817	0.000201	-0.007766	-0.008381
$4p_{3/2}$	-0.000738	0.000167	-0.007514	-0.008084
$4d_{3/2}$	-0.000820	0.000325	-0.008110	-0.008605
$4d_{5/2}$	-0.000822	0.000256	-0.008057	-0.008623
$4f_{5/2}$	-0.000607	0.000364	-0.004863	-0.005107
$4f_{7/2}$	-0.000508	0.000250	-0.004668	-0.004926

$+E^{(1)}+B^{(1)}$, the second-order Coulomb energy $E^{(2)}$, the second-order Breit correction $B^{(2)}$, the QED correction E_{Lamb}, and the total theoretical energy $E^{(\mathrm{tot})}$. The QED correction is approximated as the sum of the one-electron self-energy and the first-order vacuum-polarization energy. The vacuum-polarization contribution is calculated from the Uehling potential using the results of Fullerton and Rinker [21]. The self-energy contribution is estimated for s, $p_{1/2}$, and $p_{3/2}$ orbitals by interpolating among the values obtained by Mohr [22] using Coulomb wave functions. For this purpose, an effective nuclear charge Z_{eff} is obtained by finding the value of Z_{eff} required to give a Coulomb orbital with the same average $\langle r\rangle$ as the DHF orbital.

D. Radiative transitions to the ground state

The first-order reduced multipole matrix element $Z_K^{(1)}$ for a transition between the ground state $|0\rangle$ and the uncoupled particle-hole state $\Phi_{JM}(av)$ of Eq. (2.1) is

$$Z_K^{(1)}[0-av(J)]=\frac{1}{\sqrt{2J+1}}Z_J(av)\,\delta_{JK}. \qquad (2.13)$$

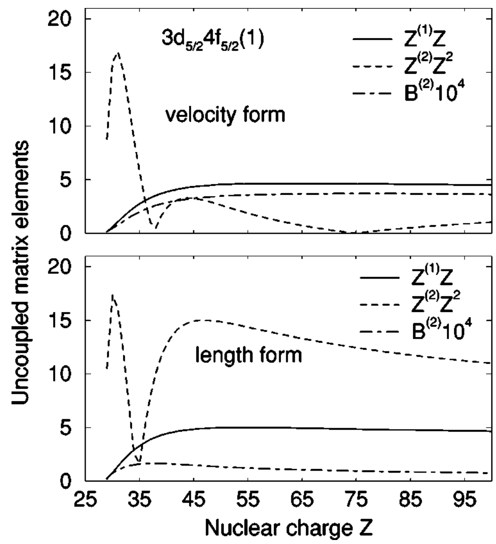

FIG. 1. Uncoupled matrix element for the transition between the $3d_{5/2}4f_{5/2}(1)$ state and the ground state calculated in length and velocity forms in Ni-like ions.

The multipole matrix $Z_K(av)$ element, which includes retardation, can be expressed in terms of the operator $t_K^{(1)}$ given in length and velocity forms by Eqs. (38) and (39), respectively, of Ref. [23] by

$$Z_K(av)=\frac{(2K+1)!!}{k^K}\langle a\|t_K^{(1)}\|v\rangle.$$

The second-order reduced matrix element $Z_K^{(2)}[0-av(J)]$ consists of three contributions: $Z_K^{(\mathrm{RPA})}$, $Z_K^{(\mathrm{HF})}$, and $Z_K^{(\mathrm{derv})}$:

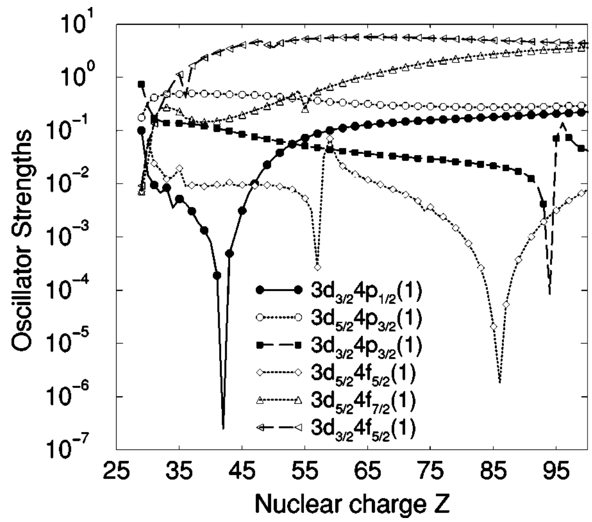

FIG. 2. Oscillator strengths for transitions between the ground state and $3d_j4p_{j'}(1)$ and $3d_j4f_{j'}(1)$ states as functions of Z.

TABLE III. Diagonal contributions to the second-order interaction term in the effective Hamiltonian matrix from diagrams R_1–R_4 calculated using HF orbitals. These contributions are given for a hole-particle ion with a $1s^2 2s^2 2p^6 3s^2 3p^6 3d^{10}$ core, and evaluated numerically for the odd-parity states with $J=1$ in the case of barium $Z=56$.

	(a) Coulomb interaction:				
	R_1^{HF}	R_2^{HF}	R_3^{HF}	R_4^{HF}	Σ^{HF}
$3d_{3/2}4p_{1/2}$	0.004141	0.002838	0.043857		0.050836
$3d_{5/2}4p_{3/2}$	0.004393	0.001551	0.038373		0.044317
$3d_{3/2}4p_{3/2}$	0.006225	0.006121	0.035867		0.048214
$3d_{5/2}4f_{5/2}$	0.005785	-0.000332	0.016577		0.022030
$3d_{5/2}4f_{7/2}$	0.005985	-0.000745	-0.016659		-0.011419
$3d_{3/2}4f_{5/2}$	0.005051	-0.001003	-0.004367		-0.000318
$3p_{3/2}4s_{1/2}$	0.002132	0.001742	0.034175		0.038050
$3p_{1/2}4s_{1/2}$	0.002421	0.003474	0.031964		0.037859
$3p_{3/2}4d_{3/2}$	0.003810	0.005657	-0.028107		-0.018640
$3p_{3/2}4d_{5/2}$	0.003907	0.006070	0.032414		0.042391
$3p_{1/2}4d_{3/2}$	0.002710	0.005221	0.034010		0.041942
$3s_{1/2}4p_{1/2}$	0.002057	0.003950	0.031657		0.037666
$3s_{1/2}4p_{3/2}$	0.001395	0.002152	0.030924		0.034470
	(b) Breit corrections:				
	R_1^{BHF}	R_2^{BHF}	R_3^{BHF}	R_4^{BHF}	Σ^{BHF}
$3d_{3/2}4p_{1/2}$	-0.000029	-0.000008	0.000130	0.002129	0.002222
$3d_{5/2}4p_{3/2}$	-0.000018	-0.000022	0.000174	0.001556	0.001632
$3d_{3/2}4p_{3/2}$	0.000012	-0.000023	0.000224	0.001654	0.001865
$3d_{5/2}4f_{5/2}$	0.000003	0.000006	0.000272	0.001054	0.001335
$3d_{5/2}4f_{7/2}$	-0.000058	-0.000005	0.000237	0.001019	0.001194
$3d_{3/2}4f_{5/2}$	-0.000027	-0.000013	0.000217	0.001248	0.001424
$3p_{3/2}4s_{1/2}$	-0.000003	-0.000007	0.000013	0.001364	0.001395
$3p_{1/2}4s_{1/2}$	0.000017	0.000023	-0.000038	0.001553	0.001555
$3p_{3/2}4d_{3/2}$	0.000001	-0.000016	-0.000261	0.001561	0.001285
$3p_{3/2}4d_{5/2}$	0.000006	-0.000006	0.000060	0.001172	0.001234
$3p_{1/2}4d_{3/2}$	-0.000007	-0.000028	0.000076	0.001566	0.001707
$3s_{1/2}4p_{1/2}$	0.000015	0.000011	0.000072	0.002074	0.002173
$3s_{1/2}4p_{3/2}$	0.000001	0.000002	0.000049	0.001410	0.001553

$$Z_K^{(\mathrm{RPA})}[0-av(J)] = \frac{1}{\sqrt{2J+1}}\,\delta_{JK}(-1)^{j_b+j_n+K}\frac{1}{2K+1} \times \sum_{b,n}\left[\frac{Z_K(bn)Z_K(anvb)}{\varepsilon_{bv}-\varepsilon_{na}} + \frac{Z_K(abvn)Z_K(nb)}{\varepsilon_{ba}-\varepsilon_{nv}}\right], \tag{2.14}$$

$$Z_K^{(\mathrm{HF})}[0-av(J)] = \frac{1}{\sqrt{2J+1}}\,\delta_{JK}\sum_n\left[\frac{Z_K(an)\Delta(nv)}{\varepsilon_v-\varepsilon_n} + \frac{\Delta(na)Z_K(nv)}{\varepsilon_a-\varepsilon_n}\right]. \tag{2.15}$$

The derivative term

$$Z_K^{(\mathrm{derv})}(av) = \frac{(2K+1)!!}{k^{K-1}}\langle a\|dt_K^{(1)}/dk\|v\rangle$$

is just the derivative of the first-order matrix element with respect to the transition energy. It is introduced to account for the first-order change in transition energy. An auxillary quantity $P_K^{(\mathrm{derv})}$ is defined by

$$P_K^{(\mathrm{derv})}[0-(av)J] = \frac{1}{\sqrt{2J+1}}Z_J^{(\mathrm{derv})}(av)\,\delta_{JK}. \tag{2.16}$$

The derivative term $Z_K^{(\mathrm{derv})}(av)$ is given in length and velocity forms by Eqs. (10) and (11) of Ref. [18] for the special case $K=1$.

The coupled dipole transition matrix element between the ground state and the Nth excited state in Ni-like ions is given by

TABLE IV. Energies of Ni-like barium for odd-parity states with $J=1$ relative to the ground state. $E^{(0+1)} \equiv E^{(0)}+E^{(1)}+B^{(1)}$.

Level	$E^{(0+1)}$	$E^{(2)}$	$B^{(2)}$	E_{LAMB}	E_{tot}
$3d_{3/2}4p_{1/2}(1)$	27.4350	-0.117082	0.032780	-0.0002	27.3505
$3d_{5/2}4p_{3/2}(1)$	27.6842	-0.111305	0.032146	0.0006	27.6056
$3d_{3/2}4p_{3/2}(1)$	28.2491	-0.119704	0.032423	0.0006	28.1624
$3d_{5/2}4f_{5/2}(1)$	34.6318	-0.130068	0.034826	0.0000	34.5366
$3d_{5/2}4f_{7/2}(1)$	35.0194	-0.162317	0.034866	0.0000	34.8919
$3d_{3/2}4f_{5/2}(1)$	35.9762	-0.159260	0.035256	0.0000	35.8522
$3p_{3/2}4s_{1/2}(1)$	34.8388	-0.208859	0.028327	0.0065	34.6648
$3p_{1/2}4s_{1/2}(1)$	37.6643	-0.236676	0.030018	0.0101	37.4677
$3p_{3/2}4d_{3/2}(1)$	41.0718	-0.266175	0.027468	-0.0031	40.8300
$3p_{3/2}4d_{5/2}(1)$	41.3278	-0.202299	0.027399	-0.0030	41.1499
$3p_{1/2}4d_{3/2}(1)$	44.0106	-0.233219	0.029421	-0.0003	43.8065
$3s_{1/2}4p_{1/2}(1)$	45.4540	-0.260963	0.027022	-0.0376	45.1825
$3s_{1/2}4p_{3/2}(1)$	46.3204	-0.258707	0.026699	-0.0377	46.0507

$$Q^{(1+2)}(0-N) = -\frac{1}{E^{(1)}[N]} \sum_{av} C_1^N[av(J)] \times \{[\epsilon_a-\epsilon_v][Z^{(1+2)}[0-av(J)] + B^{(2)}[0-av(J)]] + [-E^{(1)}[N] - \epsilon_a+\epsilon_v] P_1^{(\mathrm{derv})}[0-av(J)]\}. \quad (2.17)$$

Here $Z^{(1+2)}=Z_1^{(1)}+Z_1^{(\mathrm{RPA})}$. (Note that $Z_1^{(\mathrm{HF})}$ vanishes since we start from a HF basis.) In Eq. (2.17), we let $B^{(2)} = B_1^{(\mathrm{RPA})}+B_1^{(\mathrm{HF})}$ represent second-order corrections arising from the Breit interaction. Using the above formulas and the results for uncoupled reduced matrix elements, we transform from uncoupled reduced matrix elements to intermediate coupled matrix elements between physical states.

The uncoupled reduced matrix elements are calculated in both length and velocity gauges. The differences between length and velocity forms are illustrated for the uncoupled $0\text{-}3d_{5/2}4f_{5/2}(1)$ matrix element in Fig. 1. It should be noted that the first-order matrix element $Z^{(1)}$ is proportional 1/Z, the second-order Coulomb matrix element $Z^{(2)}$ is proportional $1/Z^2$, and the second-order Breit matrix element $B^{(2)}$ is almost independent of Z (see Ref. [18]). Taking into account this dependence, $Z^{(1)}\times Z$, $Z^{(2)}\times Z^2$, and $B^{(2)}\times 10^4$ are shown in the figure. These Z dependencies apply to the first-order matrix elements $Z^{(2)}$, the second-order matrix elements $B^{(2)}$, and the length form of $Z^{(2)}$ for high-Z ions. The contribution of the second-order matrix elements $Z^{(2)}$ is much larger in length form (compare the upper and lower panels in Fig. 1). The differences between results in length and velocity forms shown in Fig. 1 are compensated for by "derivative terms" $P^{(\mathrm{derv})}$, as shown below. It should be noted that $P^{(\mathrm{derv})}$ in the length form almost equals $Z^{(1)}$ in length form, whereas $P^{(\mathrm{derv})}$ in velocity form is smaller than $Z^{(1)}$ in velocity form by 3–4 orders of magnitude.

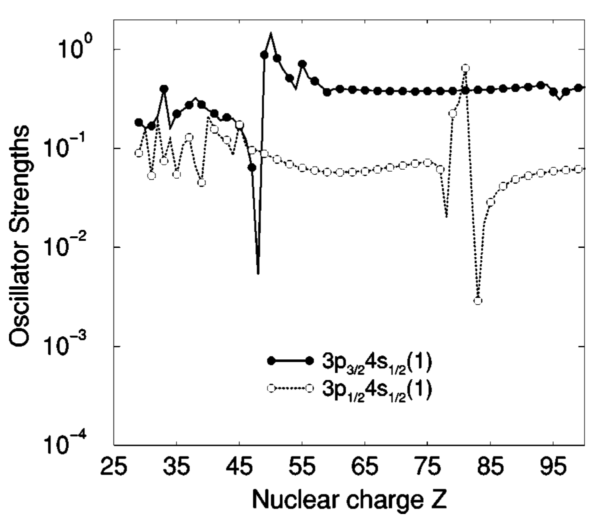

FIG. 3. Oscillator strengths for transitions between the ground state and the $3p_j4s_{1/2}(1)$ state as functions of Z.

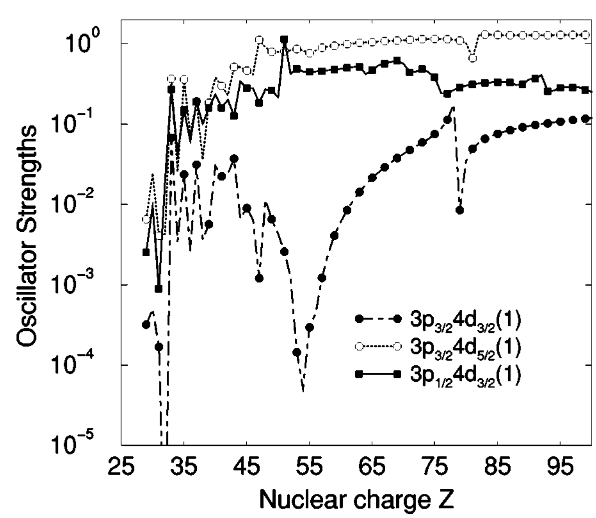

FIG. 4. Oscillator strengths for transitions between the ground state and the $3p_j4d_{j'}(1)$ state as functions of Z.

TABLE V. Uncoupled reduced matrix elements in length L and velocity V forms for odd-parity transitions into the ground state in Ba^{28+}.

$av(J)$	$Z_L^{(1)}$	$Z_V^{(1)}$	$Z_L^{(2)}$	$Z_V^{(2)}$	$B_L^{(2)}$	$B_V^{(2)}$	$P_L^{(\mathrm{derv})}$	$P_V^{(\mathrm{derv})}$
$3d_{3/2}4p_{1/2}(1)$	0.087181	0.079272	0.005138	0.005673	-0.000038	0.000008	0.086926	-0.000095
$3d_{5/2}4p_{3/2}(1)$	-0.105881	-0.096128	-0.007742	-0.007772	0.000020	0.000082	-0.105616	-0.000034
$3d_{3/2}4p_{3/2}(1)$	0.033251	0.030293	0.002660	0.002629	0.000039	0.000083	0.033096	-0.000125
$3d_{5/2}4f_{5/2}(1)$	-0.089282	-0.082514	0.005098	0.001230	-0.000167	-0.000413	-0.089265	-0.000262
$3d_{5/2}4f_{7/2}(1)$	0.398233	0.368124	-0.022676	-0.005350	0.000595	0.000771	0.396790	-0.001555
$3d_{3/2}4f_{5/2}(1)$	-0.327081	-0.302570	0.019714	0.005423	-0.000652	-0.000891	-0.326200	0.000650
$3p_{3/2}4s_{1/2}(1)$	0.104004	0.095354	0.006651	0.007440	0.000296	0.000261	0.103625	-0.000037
$3p_{1/2}4s_{1/2}(1)$	0.059547	0.054720	0.006430	0.006460	0.000338	0.000346	0.059176	-0.000231
$3p_{3/2}4d_{3/2}(1)$	0.061075	0.056603	-0.047905	-0.042744	0.000015	0.000116	0.060873	0.000052
$3p_{3/2}4d_{5/2}(1)$	0.176578	0.163864	0.009530	0.011907	0.000725	0.000955	0.175458	-0.000874
$3p_{1/2}4d_{3/2}(1)$	-0.115357	-0.107008	-0.004076	-0.005727	-0.003080	-0.002986	-0.114678	0.000345
$3s_{1/2}4p_{1/2}(1)$	0.070764	0.065459	-0.003999	-0.002890	-0.000492	-0.000343	0.070340	-0.000099
$3s_{1/2}4p_{3/2}(1)$	-0.082047	-0.075991	0.000546	0.000096	0.000138	-0.000083	-0.081292	0.000477

E. Example: Dipole matrix elements in Ba^{28+}

In Table V, we list values of *uncoupled* first- and second-order dipole matrix elements $Z^{(1)}$, $Z^{(2)}$, and $B^{(2)}$, together with derivative terms $P^{(\mathrm{derv})}$ for Ni-like barium, $Z=56$. For simplicity, we only list values for the 13 dipole transitions between odd-parity states with $J=1$ and the ground state. The derivative terms shown in Table II arise because transition amplitudes depend on energy, and the transition energy changes order-by-order in MBPT calculations. Both length (L) and velocity (V) forms are given for the matrix elements. We can see that the first-order matrix elements $Z_L^{(1)}$ and $Z_V^{(1)}$ differ by 10–20 %; the L-V differences between second-order matrix elements are much larger for some transitions as seen by comparing $Z_L^{(2)}$ and $Z_V^{(2)}$. It can also seen from Table V that $P^{(\mathrm{derv})}$ in length form almost equals $Z^{(1)}$ in length form but that $P^{(\mathrm{derv})}$ in velocity form is smaller than $Z^{(1)}$ in velocity form by 3–4 orders of magnitude.

Values of *coupled* reduced matrix elements in length and velocity forms are given in Table VI for the transitions considered in Table V. Although we use an intermediate-coupling scheme, it is nevertheless convenient to label the physical states using the jj scheme. We see that L and V forms of the coupled matrix elements in Table VI differ only in the fourth or fifth digits. These L-V differences arise because we start our MBPT calculations using a non-local Dirac-Fock (DF) potential. If we were to replace the DF potential by a local potential, the differences would disappear completely. The last two columns in Table VI show L and V values of *coupled* reduced matrix elements calculated without the second-order contribution. As can be seen from this table, removing the second-order contribution increases the L-V differences.

It should be emphasized that we include negative-energy-state (NES) contributions to sums over intermediate states. Ignoring the NES contributions leads to small changes in the L-form matrix elements, but substantial changes in some of the V-form matrix elements, with a consequent loss of gauge independence.

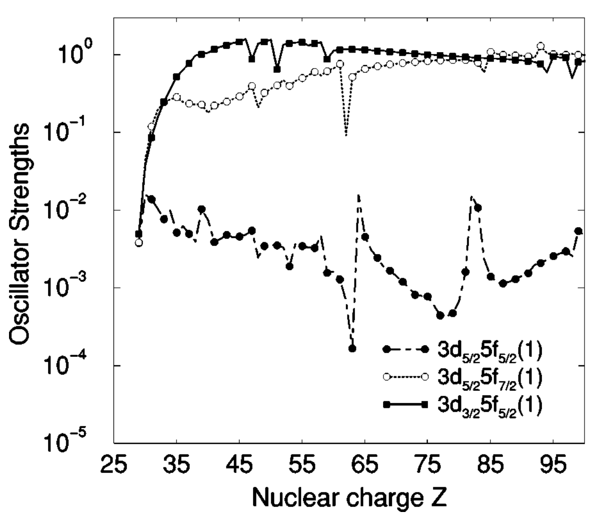

FIG. 5. Oscillator strengths for transitions between the ground state and the $3d_j5f_{j'}(1)$ state as functions of Z.

TABLE VI. Coupled reduced matrix elements in length L and velocity V forms for odd-parity transitions into the ground state in Ba^{28+}.

	MBPT		First order	
$av(J)$	L	V	L	V
$3d_{3/2}4p_{1/2}(1)$	-0.068287	-0.067912	-0.064126	-0.058401
$3d_{5/2}4p_{3/2}(1)$	-0.140705	-0.140013	-0.132503	-0.120496
$3d_{3/2}4p_{3/2}(1)$	0.050965	0.050680	0.047335	0.043148
$3d_{5/2}4f_{5/2}(1)$	-0.011981	-0.011825	-0.011005	-0.010230
$3d_{5/2}4f_{7/2}(1)$	-0.145601	-0.145668	-0.154598	-0.142856
$3d_{3/2}4f_{5/2}(1)$	0.467167	0.467484	0.496550	0.459288
$3p_{3/2}4s_{1/2}(1)$	0.148537	0.148052	0.144775	0.133128
$3p_{1/2}4s_{1/2}(1)$	-0.051011	-0.050367	-0.041079	-0.037665
$3p_{3/2}4d_{3/2}(1)$	0.046451	0.042222	-0.003995	-0.003625
$3p_{3/2}4d_{5/2}(1)$	0.170504	0.170879	0.176448	0.163761
$3p_{1/2}4d_{3/2}(1)$	0.124708	0.123974	0.115723	0.107345
$3s_{1/2}4p_{1/2}(1)$	-0.040535	-0.040678	-0.043162	-0.039890
$3s_{1/2}4p_{3/2}(1)$	-0.062830	-0.063085	-0.065063	-0.060257

TABLE VII. Wavelengths (λ in Å) for Ni-like ions for odd-parity states with $J=1$ given relative to the ground state. Comparison with experimental results presented in Refs. [10], [11], and [14].

	$3d_{3/2}4p_{1/2}$	$3d_{5/2}4p_{3/2}$	$3d_{3/2}4p_{3/2}$	$3d_{5/2}4f_{5/2}$	$3d_{5/2}4f_{7/2}$	$3d_{3/2}4f_{5/2}$	$3p_{3/2}4s_{1/2}$	$3p_{1/2}4s_{1/2}$	$3p_{3/2}4d_{3/2}$	$3p_{3/2}4d_{5/2}$	$3p_{1/2}4d_{3/2}$
$Z=47$	31.491	31.242	30.812	23.601	23.397	22.852	22.561	21.329	18.814	18.706	17.888
λ_{expt} [14]	31.427	31.189	30.757	23.571	23.333	22.821					
$Z=48$	28.986	28.760	28.345	21.897	21.704	21.187	21.069	19.914	17.612	17.512	16.713
λ_{expt} [14]	28.934	28.716	28.301	21.970	21.450	21.160					
$Z=49$	26.777	26.570	26.169	20.379	20.196	19.727	19.702	18.593	16.516	16.428	15.657
λ_{expt} [14]	26.735	26.533	26.131		20.040	19.710					
$Z=50$	24.820	24.627	24.238	19.020	18.846	18.359	18.527	17.402	15.541	15.450	14.692
λ_{expt} [14]	24.785	24.596	24.211	19.027	18.811	18.356					
$Z=51$	23.076	22.894	22.522	17.798	17.633	17.176	17.414	16.321	14.640	14.554	13.814
$Z=52$	21.516	21.342	20.981	16.694	16.537	16.106	16.403	15.337	13.818	13.736	13.011
$Z=53$	20.113	19.946	19.595	15.694	15.543	15.135	15.480	14.438	13.064	12.985	12.275
$Z=54$	18.847	18.686	18.339	14.784	14.639	14.252	14.634	13.614	12.371	12.295	11.600
λ_{expt} [14]	18.826	18.667	18.326		14.618						
$Z=55$	17.701	17.544	17.210	13.953	13.813	13.446	13.859	12.857	11.727	11.659	10.977
$Z=56$	16.659	16.505	16.179	13.193	13.058	12.709	13.144	12.161	11.159	11.072	10.401
λ_{expt} [10]					13.046	12.721	13.136		11.072	10.388	
$Z=57$	15.709	15.558	15.239	12.495	12.365	12.032	12.484	11.518	10.600	10.503	9.868
λ_{expt} [11]					12.335	12.020	12.458		10.512	9.841	
$Z=58$	14.841	14.692	14.379	11.856	11.727	11.409	11.870	10.923	10.093	10.027	9.374
$Z=59$	14.045	13.897	13.591	11.257	11.138	10.834	11.310	10.372	9.622	9.557	8.915
λ_{expt} [11]				11.256	11.129	10.842	11.310			9.559	8.915
$Z=60$	13.313	13.167	12.866	10.709	10.594	10.303	10.785	9.861	9.184	9.121	8.487
$Z=61$	12.639	12.493	12.199	10.201	10.089	9.810	10.296	9.385	8.775	8.713	8.088
$Z=62$	12.016	11.871	11.580	9.729	9.620	9.352	9.841	8.941	8.393	8.333	7.716
λ_{expt} [14]	11.950	11.830	11.530	9.785	9.620		9.850				
$Z=63$	11.440	11.295	11.011	9.289	9.184	8.926	9.417	8.527	8.036	7.976	7.367
$Z=64$	10.905	10.761	10.479	8.880	8.777	8.529	9.020	8.140	7.701	7.642	7.040
λ_{expt} [14]	10.900	10.750	10.470		8.770	8.530	9.010			7.638	
$Z=65$	10.409	10.265	9.989	8.497	8.398	8.158	8.648	7.778	7.387	7.329	6.734
$Z=66$	9.947	9.803	9.529	8.139	8.043	7.811	8.299	7.438	7.091	7.034	6.446
λ_{expt} [14]	9.960	9.810	9.540		8.020	7.820	8.280				
$Z=67$	9.516	9.372	9.103	7.804	7.710	7.486	7.972	7.119	6.813	6.757	6.175
$Z=68$	9.113	8.969	8.704	7.489	7.398	7.181	7.665	6.819	6.551	6.495	5.920
$Z=69$	8.737	8.592	8.329	7.193	7.104	6.894	7.375	6.537	6.304	6.249	5.678
λ_{expt} [14]	8.734	8.591	8.326	7.184	7.099	6.890	7.370	6.528	6.296	6.245	5.655
$Z=70$	8.384	8.239	7.979	6.915	6.829	6.624	7.103	6.270	6.071	6.016	5.459
λ_{expt} [14]	8.377	8.235	7.978	6.914	6.822	6.620	7.099	6.270	6.061	6.01	5.44
$Z=71$	8.053	7.908	7.652	6.653	6.569	6.369	6.845	6.019	5.850	5.795	5.205
$Z=72$	7.743	7.596	7.342	6.406	6.323	6.129	6.603	5.782	5.641	5.587	5.006
λ_{expt} [14]	7.739	7.594	7.339	6.419	6.317	6.125	6.596	5.780	5.640	5.586	
$Z=73$	7.450	7.303	7.052	6.172	6.092	5.902	6.373	5.558	5.443	5.389	4.816
λ_{expt} [14]	7.447	7.301	7.051	6.176	6.092	5.907	6.370		5.43	5.382	4.818
$Z=74$	7.175	7.027	6.779	5.951	5.873	5.687	6.156	5.345	5.255	5.202	4.635
λ_{expt} [14]	7.172	7.024	6.775	5.956	5.871	5.689	6.154		5.247	5.200	4.638
$Z=75$	6.916	6.767	6.521	5.742	5.666	5.484	5.950	5.144	5.077	5.024	4.463
λ_{expt} [14]	6.914	6.765	6.518	5.740	5.663	5.484	5.943			5.025	4.464
$Z=76$	6.671	6.521	6.278	5.544	5.470	5.292	5.755	4.953	4.907	4.854	4.298
$Z=77$	6.440	6.289	6.048	5.356	5.284	5.109	5.570	4.773	4.745	4.693	4.142
$Z=78$	6.221	6.069	5.829	5.178	5.107	4.936	5.394	4.588	4.604	4.540	3.992
λ_{expt} [14]	6.214	6.062	5.824	5.179	5.098	4.932				4.539	3.993

TABLE VII. (*Continued*).

	$3d_{3/2}4p_{1/2}$	$3d_{5/2}4p_{3/2}$	$3d_{3/2}4p_{3/2}$	$3d_{5/2}4f_{5/2}$	$3d_{5/2}4f_{7/2}$	$3d_{3/2}4f_{5/2}$	$3p_{3/2}4s_{1/2}$	$3p_{1/2}4s_{1/2}$	$3p_{3/2}4d_{3/2}$	$3p_{3/2}4d_{5/2}$	$3p_{1/2}4d_{3/2}$
$Z=79$	6.014	5.860	5.623	5.009	4.939	4.771	5.227	4.430	4.452	4.394	3.850
λ_{expt} [14]	6.010	5.850	5.620		4.930	4.760	5.222				3.851
$Z=80$	5.818	5.663	5.427	4.847	4.780	4.614	5.068	4.277	4.309	4.254	3.714
λ_{expt} [14]	5.816	5.657	5.417		4.771	4.609	5.055			4.252	3.714
$Z=81$	5.632	5.475	5.243	4.694	4.628	4.464	4.916	4.131	4.176	4.119	3.584
$Z=82$	5.455	5.297	5.065	4.548	4.483	4.322	4.772	3.984	4.049	3.998	3.461
λ_{expt} [14]	5.454	5.291	5.055		4.475	4.318	4.759			3.998	
$Z=83$	5.287	5.128	4.898	4.409	4.345	4.186	4.635	3.849	3.927	3.875	3.342
$Z=84$	5.128	4.967	4.739	4.276	4.214	4.056	4.504	3.720	3.811	3.759	3.230
$Z=85$	4.976	4.813	4.587	4.149	4.088	3.933	4.379	3.597	3.700	3.648	3.119
$Z=86$	4.832	4.667	4.442	4.027	3.968	3.814	4.260	3.479	3.594	3.542	3.015
$Z=87$	4.694	4.527	4.304	3.911	3.853	3.701	4.145	3.365	3.492	3.440	2.916
$Z=88$	4.563	4.394	4.172	3.800	3.743	3.593	4.036	3.257	3.394	3.342	2.820
$Z=89$	4.438	4.266	4.046	3.694	3.638	3.489	3.932	3.153	3.300	3.249	2.728
$Z=90$	4.319	4.145	3.925	3.592	3.537	3.389	3.832	3.053	3.210	3.159	2.640
$Z=91$	4.205	4.028	3.810	3.494	3.441	3.294	3.737	2.957	3.124	3.073	2.555
$Z=92$	4.096	3.917	3.700	3.401	3.348	3.202	3.645	2.865	3.041	2.990	2.474

III. X-RAY WAVELENGTHS FOR NI-LIKE IONS $Z=47-92$

The $n=3-4$ transitions in Ni-like ions have been thoroughly investigated, theoretically and experimentally. In Table VII, our MBPT results of wavelengths for transitions from 11 excited $J=1$ states to the ground state are compared with experimental data given in Refs. [10], [11], and [14]. Other references to experimental measurements were omitted since they were included by Quinet and Biémont in Ref. [14]. The $n=3-4$ transitions observed in x-ray spectra of the Ni-like ions Ag^{19+}-Pb^{54+} were investigated theoretically in Ref. [14] using the multiconfigurational Dirac-Fock approach. Our MBPT method starts from the Dirac-Fock approximation, and includes correlation corrections for Coulomb-Coulomb ($E^{(2)}$) and Coulomb-Breit $B^{(2)}$) interactions. The correlation corrections are in the range 2000–10 000 cm^{-1}, as seen in Table IV. Consequently, our MBPT data in Table VII are in closer agreement with experimental data than the uncorrelated values from Ref. [14], and can be used to predict wavelengths in future experiments.

TABLE VIII. Wavelengths (λ in Å) for $3d4p(J)$-$3d4d(J')$ transitions in Ni-like ions. Comparison with experimental data (λ_{expt}) and predicted data (λ_{fit}) from Scofield and MacGowan in Ref. [5].

	$3d_{5/2}4p_{3/2}(1)$-$3d_{5/2}4d_{5/2}(2)$			$3d_{5/2}4p_{3/2}(1)$-$3d_{5/2}4d_{5/2}(1)$		
Z	λ_{MBPT}	λ_{fit}	λ_{expt}	λ_{MBPT}	λ_{fit}	λ_{expt}
47	188.49	189.06		195.54	195.83	
48	179.26	179.73		186.05	186.26	
49	170.84	171.23		177.39	177.56	
50	163.15	163.49		169.47	169.58	
54	137.85	138.04		143.39	143.47	
62	103.68	103.72		108.01	108.01	
64	97.24	97.26		101.31	101.30	
66	91.38	91.38		95.21	95.19	
69	83.51	83.50		87.00	86.97	
70	81.39	81.08	81.07	84.48	84.45	84.41
72	76.81	76.53		79.73	79.69	
73	74.63	74.38	74.42	77.48	77.45	77.47
74	72.54	72.31	72.40	75.32	75.28	75.35
75	70.49	70.32		73.23	73.19	
78	64.83	64.73		67.38	67.34	
79	63.08	62.99		65.56	65.51	
80	61.39	61.30		63.79	63.74	
82	58.18	58.09		60.43	60.38	

IV. WAVELENGTHS OF TRANSITIONS BETWEEN EXCITED STATES

Transitions between excited states were studied mostly for purpose of obtaining accurate data for lasing

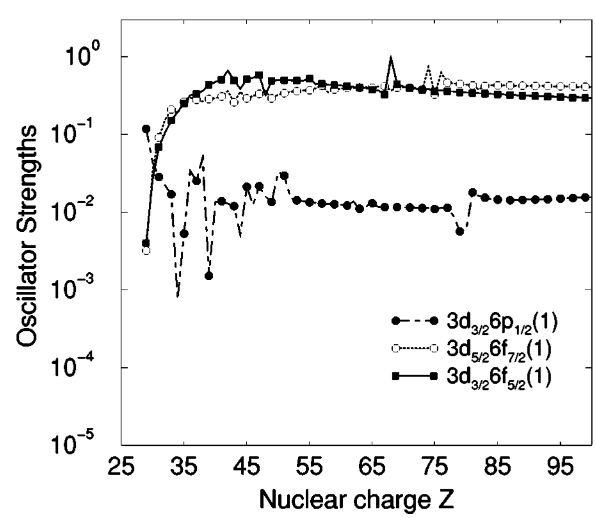

FIG. 6. Oscillator strengths for transitions between the ground state and the $3d_j6f_{j'}(1)$ state as functions of Z.

TABLE IX. Wavelengths (λ in Å) for $3d4s(J)$-$3d4p(J')$ transitions in Ni-like ions. Comparison with experimental results from Churilov *et al.* in Ref. [15].

$3dj4s(J)$	$3dj4pj'(J')$	$Z=47$		$Z=48$		$Z=49$		$Z=50$	
		$\lambda_{\rm MBPT}$	$\lambda_{\rm expt}$	$\lambda_{\rm MBPT}$	$\lambda_{\rm expt}$	$\lambda_{\rm MBPT}$	$\lambda_{\rm expt}$	$\lambda_{\rm MBPT}$	$\lambda_{\rm expt}$
$3d_{5/2}4s(3)$	$3d_{3/2}4p_{3/2}(2)$	221.856		207.389		194.109		181.878	
$3d_{5/2}4s(2)$	$3d_{3/2}4p_{3/2}(2)$	225.089		210.357		196.817		184.358	
$3d_{5/2}4s(3)$	$3d_{3/2}4p_{3/2}(3)$	227.142		212.179		198.446		185.809	
$3d_{5/2}4s(2)$	$3d_{3/2}4p_{3/2}(1)$	229.072		214.124		200.348		187.676	
$3d_{5/2}4s(2)$	$3d_{3/2}4p_{3/2}(3)$	230.532		215.287		201.277		188.398	
$3d_{5/2}4s(3)$	$3d_{5/2}4p_{3/2}(3)$	248.581	248.745	233.874	234.043	220.335	220.593	207.828	207.988
$3d_{3/2}4s(1)$	$3d_{3/2}4p_{3/2}(2)$	250.082	250.292	235.299	235.536	221.697	221.977	209.115	209.288
$3d_{5/2}4s(2)$	$3d_{5/2}4p_{3/2}(3)$	252.647	252.820	237.656	237.859	223.831	224.106	211.072	
$3d_{3/2}4s(2)$	$3d_{3/2}4p_{3/2}(2)$	253.505	253.685	238.402	238.614	224.515	224.745	211.689	211.845
$3d_{5/2}4s(3)$	$3d_{5/2}4p_{3/2}(2)$	253.505		238.601		224.859		212.143	
$3d_{3/2}4s(1)$	$3d_{3/2}4p_{3/2}(1)$	255.008	254.992	240.022	240.074	226.187	226.242	213.395	
$3d_{5/2}4s(2)$	$3d_{5/2}4p_{3/2}(1)$	255.165	240.258	240.288	226.430	226.524	213.631	213.765	
$3d_{5/2}4s(2)$	$3d_{5/2}4p_{3/2}(2)$	257.735	258.045	242.539	242.817	228.501	228.802	215.525	215.745
$3d_{3/2}4s(2)$	$3d_{3/2}4p_{3/2}(1)$	258.568		243.251		229.122		216.077	
$3d_{3/2}4s(2)$	$3d_{3/2}4p_{3/2}(3)$	260.430	260.485	244.754	244.850	230.338	230.478	217.034	217.135
$3d_{5/2}4s(3)$	$3d_{5/2}4p_{3/2}(4)$	260.759	260.875	245.096	245.222	230.687	230.895	217.386	217.493
$3d_{3/2}4s(1)$	$3d_{3/2}4p_{3/2}(0)$	270.031	270.010	253.609	253.677	238.513	238.777	224.575	
$3d_{5/2}4s(3)$	$3d_{3/2}4p_{1/2}(2)$	272.258	272.133	256.999		242.951		229.995	
$3d_{5/2}4s(2)$	$3d_{3/2}4p_{1/2}(1)$	272.795	272.133	257.028	256.410	242.577		229.299	
$3d_{5/2}4s(2)$	$3d_{3/2}4p_{1/2}(2)$	277.143		261.573		247.209		233.975	
$3d_{3/2}4s(1)$	$3d_{5/2}4p_{3/2}(1)$	287.767		273.391		260.122		247.779	247.920
$3d_{3/2}4s(2)$	$3d_{5/2}4p_{3/2}(3)$	289.009		274.081		260.360		247.685	
$3d_{3/2}4s(1)$	$3d_{5/2}4p_{3/2}(2)$	291.039	291.713	276.309		262.732		250.146	250.780
$3d_{3/2}4s(2)$	$3d_{5/2}4p_{3/2}(1)$	292.309	292.568	277.588	277.851	264.011	264.206	251.402	251.524
$3d_{3/2}4s(2)$	$3d_{5/2}4p_{3/2}(2)$	295.686		280.597		266.700		253.839	
$3d_{3/2}4s(1)$	$3d_{3/2}4p_{1/2}(1)$	310.390		295.272		281.514		268.895	
$3d_{5/2}4s(3)$	$3d_{5/2}4p_{1/2}(3)$	310.856	311.039	296.443	296.622	283.247	283.448	271.071	271.264
$3d_{3/2}4s(2)$	$3d_{3/2}4p_{1/2}(1)$	315.680	315.041	300.174	299.660	286.075	285.667	273.167	
$3d_{3/2}4s(1)$	$3d_{3/2}4p_{1/2}(2)$	316.031	315.952	301.285	301.276	287.772	287.791	275.346	275.368
$3d_{5/2}4s(2)$	$3d_{5/2}4p_{1/2}(3)$	317.241	317.408	302.545	302.800	289.051	289.298	276.617	276.809
$3d_{5/2}4s(3)$	$3d_{5/2}4p_{1/2}(2)$	318.105	317.932	303.089	302.972	289.363	289.298	276.735	276.651
$3d_{3/2}4s(2)$	$3d_{3/2}4p_{1/2}(2)$	321.517		306.390	306.315	292.540		279.828	
$3d_{5/2}4s(2)$	$3d_{5/2}4p_{1/2}(2)$	324.793		309.471	309.390	295.423		282.517	
$3d_{3/2}4s(2)$	$3d_{5/2}4p_{1/2}(3)$	376.763		364.157		353.010		343.080	
$3d_{3/2}4s(1)$	$3d_{5/2}4p_{1/2}(2)$	379.524		366.648		355.266		345.133	
$3d_{3/2}4s(2)$	$3d_{5/2}4p_{1/2}(2)$	387.463		374.237		362.561		352.203	

lines. In Table VIII, our MBPT wavelengths for the two lasing lines $3d_{5/2}4p_{3/2}(1)$-$3d_{5/2}4d_{5/2}(2)$ and $3d_{5/2}4p_{3/2}(1)$-$3d_{5/2}4d_{5/2}(1)$ are compared with predicted and experimental values given by Scofield and MacGowan in Ref. [5] for ions in the range $Z=47$–82. The prediction in Ref. [5] was obtained by a semiempirical fit to the experimental measurement given in Table VIII.

Our MBPT calculations are in a good agreement with the three experimental values and with predicted data in interval $Z=62$–82 for the $3d_{5/2}4p_{3/2}(1)$-$3d_{5/2}4d_{5/2}(1)$ line. There is also a good agreement with predicted data for the $3d_{5/2}4p_{3/2}(1)$–$3d_{5/2}4d_{5/2}(2)$ line in intervals $Z=62$–69 and 78–82. However our MBPT calculations for this line disagrees with experimental and predicted data in the range of $Z=70$–73. We have no explanation for this disagreement.

In Table IX, our MBPT results of wavelengths for $3d_{j_1}4s_{1/2}(J)$-$3d_{j_2}4p_j(J')$ transitions are compared with experimental data given in Ref. [15]. The identification given in Ref. [15] for $\Delta n=0$ transitions in the spectra of four Ni-like ions with $Z=47$–50 was based on the Slater-Condon method with generalized least-square (GLS) fits of energy parameters. This method was described by Wyart [16]. As can be seen from Table IX, our MBPT data are in a good agreement with experimental data: the disagreement in $3d_{j_1}4s_{1/2}(J)$-$3d_{j_2}4p_j(J')$ wavelengths is about 0.07%, except for three lines [$3d_{5/2}4s_{1/2}(2)$-$3d_{3/2}4p_{1/2}(1)$ in Cd^{20+}, $3d_{3/2}4s_{1/2}(2)$-$3d_{3/2}4p_{1/2}(1)$ in In^{21+}, and

TABLE X. Wavelengths (λ in Å) for $3d4p(J)$-$3d4d(J')$ transitions in Ni-like ions. Comparison with experimental data (λ_{expt}) from Churilov *et al.* in Ref. [15] and predicted data (λ_{GLS}) from Wyart in Ref. [16].

$3dj4pj'(J)$	$3dj4pj'(J')$	$Z=47$		$Z=48$		$Z=49$		$Z=50$	
		λ_{MBPT}	λ_{GLS}	λ_{MBPT}	λ_{GLS}	λ_{MBPT}	λ_{GLS}	λ_{MBPT}	λ_{GLS}
$3d_{5/2}4p_{1/2}(3)$	$3d_{5/2}4d_{5/2}(4)$	164.228		154.962		146.459		138.630	
$3d_{3/2}4p_{1/2}(2)$	$3d_{3/2}4d_{5/2}(2)$	164.631		155.406		146.931		139.112	
$3d_{5/2}4p_{1/2}(3)$	$3d_{5/2}4d_{5/2}(2)$	164.685		155.400		146.879		139.036	
$3d_{3/2}4p_{1/2}(2)$	$3d_{3/2}4d_{3/2}(2)$	165.318	165.336	156.323	156.303	148.082	148.010	140.480	140.360
$3d_{5/2}4p_{1/2}(3)$	$3d_{5/2}4d_{5/2}(3)$	165.878	165.635	156.521	156.217	147.938	147.567	140.031	139.588
$3d_{5/2}4p_{1/2}(2)$	$3d_{5/2}4d_{3/2}(3)$	166.752	166.845	157.675	157.717	149.354	149.333	141.677	141.600
$3d_{3/2}4p_{1/2}(1)$	$3d_{3/2}4d_{3/2}(2)$	166.905		157.992		149.796		142.221	
$3d_{5/2}4p_{1/2}(2)$	$3d_{5/2}4d_{5/2}(1)$	167.951		158.597		149.998		142.061	
$3d_{3/2}4p_{1/2}(2)$	$3d_{3/2}4d_{5/2}(1)$	168.304		158.907		150.280		142.305	
$3d_{5/2}4p_{1/2}(3)$	$3d_{5/2}4d_{3/2}(3)$	168.816	168.796	159.536	159.481	151.037	150.933	143.209	143.056
$3d_{5/2}4p_{1/2}(2)$	$3d_{5/2}4d_{3/2}(2)$	168.991	168.862	159.782	159.610	151.328	151.111	143.538	143.269
$3d_{3/2}4p_{1/2}(1)$	$3d_{3/2}4d_{5/2}(1)$	169.949		160.632		152.045		144.092	
$3d_{3/2}4p_{1/2}(2)$	$3d_{3/2}4d_{3/2}(3)$	170.502	170.677	161.223	161.346	152.703	152.771	144.848	144.855
$3d_{5/2}4p_{1/2}(3)$	$3d_{5/2}4d_{3/2}(2)$	171.111		161.693		153.056		145.111	
$3d_{3/2}4p_{1/2}(2)$	$3d_{3/2}4d_{3/2}(1)$	171.911		162.471		153.816		145.831	
$3d_{5/2}4p_{1/2}(3)$	$3d_{5/2}4d_{3/2}(4)$	171.963	171.798	162.529	162.323	153.873	153.624	145.906	145.602
λ_{expt}		171.987							
$3d_{3/2}4p_{1/2}(1)$	$3d_{3/2}4d_{3/2}(1)$	173.627		164.275		155.666		147.708	
$3d_{5/2}4p_{1/2}(2)$	$3d_{5/2}4d_{3/2}(1)$	176.856	176.901	167.088	167.049	158.124	157.999	149.855	149.651
$3d_{5/2}4p_{3/2}(2)$	$3d_{3/2}4d_{3/2}(3)$	178.785	178.710	169.418	169.318	160.837	160.710	152.954	152.784
$3d_{3/2}4p_{1/2}(2)$	$3d_{5/2}4d_{5/2}(3)$	179.454	179.363	170.324	170.145	161.969	161.683	154.264	153.878
$3d_{3/2}4p_{1/2}(1)$	$3d_{5/2}4d_{5/2}(2)$	179.900	179.848	170.950	170.771	162.720	162.415	155.125	154.688
$3d_{5/2}4p_{3/2}(4)$	$3d_{5/2}4d_{5/2}(4)$	182.780	182.397	174.019	173.560	166.017	165.475	158.669	158.042
$3d_{5/2}4p_{3/2}(4)$	$3d_{5/2}4d_{5/2}(3)$	184.826		175.988		167.920		160.508	
$3d_{3/2}4p_{3/2}(0)$	$3d_{3/2}4d_{5/2}(1)$	185.096	184.774	176.397	176.006	168.447	167.969	161.132	160.567
$3d_{3/2}4p_{3/2}(3)$	$3d_{3/2}4d_{5/2}(3)$	184.977	184.743	176.117	175.810	168.025	187.633	160.598	160.114
$3d_{3/2}4p_{3/2}(3)$	$3d_{3/2}4d_{5/2}(2)$	187.103		178.163		169.987		162.482	
$3d_{5/2}4p_{3/2}(2)$	$3d_{5/2}4d_{5/2}(2)$	187.111	186.658	178.024	177.495	169.734	169.120	162.136	161.430
$3d_{3/2}4p_{3/2}(3)$	$3d_{3/2}4d_{3/2}(2)$	187.991		179.369		171.530		164.352	
$3d_{3/2}4p_{3/2}(1)$	$3d_{3/2}4d_{5/2}(2)$	188.076	187.645	178.968	178.480	170.655	170.096	163.023	162.391
$3d_{5/2}4p_{3/2}(4)$	$3d_{5/2}4d_{3/2}(3)$	188.481		179.808		171.924		164.697	
$3d_{5/2}4p_{3/2}(1)$	$3d_{5/2}4d_{5/2}(2)$	188.489		179.256		170.841		163.146	
$3d_{5/2}4p_{3/2}(2)$	$3d_{5/2}4d_{5/2}(3)$	188.653	188.255	179.496	179.034	171.149	170.603	163.491	162.857
λ_{expt}		188.590							
$3d_{3/2}4p_{3/2}(2)$	$3d_{3/2}4d_{5/2}(3)$	188.637	188.329	179.560	179.180	171.265	170.809	163.656	163.112
$3d_{3/2}4p_{3/2}(1)$	$3d_{3/2}4d_{3/2}(2)$	188.973	188.872	180.185	180.060	172.210	172.027	164.905	164.669
$3d_{3/2}4p_{3/2}(3)$	$3d_{3/2}4d_{5/2}(4)$	189.224	188.817	180.164	179.687	171.892	171.328	164.299	163.638
λ_{expt}		189.092		180.218					
$3d_{5/2}4p_{3/2}(4)$	$3d_{5/2}4d_{5/2}(5)$	189.319	188.901	180.263	179.768	171.989	171.407	164.388	163.716
λ_{expt}		189.315		180.218		172.055			
$3d_{5/2}4p_{3/2}(3)$	$3d_{5/2}4d_{5/2}(4)$	189.279	188.858	180.156	179.665	171.827	171.254	164.180	163.524
λ_{expt}		189.230		180.218					
$3d_{3/2}4p_{3/2}(0)$	$3d_{3/2}4d_{3/2}(1)$	189.468		180.800		172.903		165.667	
$3d_{5/2}4p_{3/2}(3)$	$3d_{5/2}4d_{5/2}(2)$	189.887		180.750		172.406		164.750	
$3d_{3/2}4p_{3/2}(2)$	$3d_{3/2}4d_{5/2}(2)$	190.849	190.426	181.687	181.196	173.304	172.745	165.613	164.791
$3d_{5/2}4p_{3/2}(3)$	$3d_{5/2}4d_{5/2}(3)$	191.475	191.082	182.268	181.804	173.866	173.312	166.150	165.504
$3d_{3/2}4p_{3/2}(2)$	$3d_{3/2}4d_{3/2}(2)$	191.773		182.941		174.907		167.556	
$3d_{5/2}4p_{3/2}(4)$	$3d_{5/2}4d_{3/2}(4)$	192.413		183.619		175.609		168.273	
$3d_{5/2}4p_{3/2}(2)$	$3d_{5/2}4d_{3/2}(3)$	192.462		183.472		175.311		167.839	
$3d_{3/2}4p_{3/2}(1)$	$3d_{3/2}4d_{5/2}(1)$	192.885		183.627		175.190		167.426	
$3d_{5/2}4p_{3/2}(2)$	$3d_{5/2}4d_{5/2}(1)$	194.060		184.721		176.199		168.379	
$3d_{3/2}4p_{3/2}(3)$	$3d_{3/2}4d_{3/2}(3)$	194.724		185.851		177.760		170.362	
$3d_{5/2}4p_{3/2}(3)$	$3d_{5/2}4d_{3/2}(3)$	195.400	195.302	186.369	186.240	178.163	177.973	170.643	170.401

$3d_{3/2}4s_{1/2}(1)$-$3d_{5/2}4p_{3/2}(2)$ in Sn^{22+}], where the disagreement is about 0.2%. Since the relativistic MBPT calculations are more accurate for high-Z ions, we conclude that the MBPT method provides accurate wavelengths for $3d_{j_1}4s_{1/2}(J)$-$3d_{j_2}4p_j(J')$ for ions with $Z>50$.

Only several lines for $3d_{j_1}4p_{j_2}(J)$-$3d_{j_3}4d_{j_4}(J')$ transitions were observed and identified by Churilov *et al.* [15] in Ni-like ions with $Z=47$–50. These data, together with our MBPT data and predicted theoretical data [16], are presented in Table X. The GLS label is used for data from Ref. [16], since they were determined in generalized least-squares fits using all known levels in the Ni sequence. As can be seen from Table X, our MBPT data λ_{MBPT} are in better agreement with experimental data λ_{expt} than with predicted data λ_{GLS}.

V. OSCILLATOR STRENGTHS, FOR DIPOLE TRANSITIONS TO THE GROUND STATE

As mentioned previously, line strengths, oscillator strengths, and transition rates for dipole transitions between odd-parity states with $J=1$ and the ground state are calculated in Ni-like ions with nuclear charges ranging from $Z=29$ to 100. Results are obtained in both length and velocity forms, but only length-form results are tabulated, since length-velocity differences are less than 1% for most cases.

In Figs. 2–6, we present the Z dependence of oscillator strengths of transitions from $J=1$ excited states to the ground states. The sharp features in the curves shown in these figures can be explained in many cases by the strong mixing of states inside the odd-parity complex with $J=1$. In Fig. 2, the double cusp in the interval $Z=57$–59 is due to mixing of the $3d_{5/2}4f_{5/2}(1)$ and $3d_{5/2}4f_{7/2}(1)$ states. The mixing of the $3d_{5/2}4f_{7/2}(1)$ and $3d_{3/2}4f_{5/2}(1)$ states in the $Z=55$–56 range gives a singularity in the curve with the $3d_{5/2}4f_{7/2}(1)$ label. The mixing of the $3d_{3/2}4f_{5/2}(1)$ and $3p_{3/2}4s_{1/2}(1)$ states in the $Z=49$–50 range gives a singularity in the curve with the $3d_{3/2}4f_{5/2}(1)$ label. The deep minimum in the curve with the $3d_{3/2}4p_{1/2}(1)$ label in the $Z=43$–44 range can be explained by mixing of the $3d_{3/2}4p_{1/2}(1)$ and $3d_{5/2}4p_{3/2}(1)$ states. Most of the remaining singularities in Figs. 2–6 can be explained in a similar way.

These singularities are a consequence of coupling between states governed by the first-order mixing coefficients $C_1^N[av(J)]$ in Eq. (2.17). Comparison with the MCDF oscillator strengths given in Ref. [14] confirms this conclusion. However, some of the singularities are caused by second-order uncoupled matrix elements. As can be seen from the expression for $Z_K^{(\mathrm{RPA})}$ [Eq. (2.14)], the dominator of one term is $\epsilon_{bv}-\epsilon_{na}$. When $v=4d_{5/2}$, $a=3p_{3/2}$, $n=5p_{3/2}$, and $b=3d_{5/2}$, the sign of the denominator changes sign in the interval $Z=57$–58, and the denominator becomes very small for $Z=57$. A similar situation occurs for other cases: $\epsilon_{4p_{3/2}}-\epsilon_{3s_{1/2}}+\epsilon_{3d_{5/2}}-\epsilon_{5f_{7/2}}$ changes signs in the interval $Z=66$–67, and so forth. In these cases, the contribution of the term with these small denominators becomes much larger than other contributions, leading to new singularities in the Z dependence of the oscillator strengths. We removed some of these singularities by increasing our model space to include $3d_jnp_{j'}$ and $3d_jnf_{j'}$ states with $n=5$ and 6, and simultaneously removing the states from the sum over n in the expression for $Z_K^{(\mathrm{RPA})}$ in Eq. (2.14).

As can be seen from Figs. 3 and 4, some small singularities still remain for $3p_j4s_{1/2}(1)$ states in the $Z=29$–35 range, and $3p_j4d_{j'}(1)$ in the $Z=29$–45 range. These $3p_j4s_{1/2}(1)$ and $3p_j4d_{j'}(1)$ states are autoionizing for the $3d_j$-hole threshold in the $Z=29$–35 and 29–40 ranges. In this case, the singularity is in the positive part of the spectra in the sum over n in Eq. (2.14) for $Z_K^{(\mathrm{RPA})}$. Our conclusion concerning the importance of autoionizing states in low-Z Ni-like ions for calculations of the oscillator strengths can be extended to other atomic data.

VI. CONCLUSION

In summary, a systematic second-order MBPT study of excitation energies of the 106 $3l$-$4l'$ hole-particle states of Ni-like ions was presented. Theoretical wavelengths in the x-ray spectra of Ni-like ions $Ag^{19+}-Pb^{54+}$ differ from existing experimental wavelength data at the level 0.01–0.1%. Wavelengths of $3l_14l_2(J)-3l_34l_4(J)$ transitions differ from existing experimental wavelengths for intermediate values of Z at the level 0.07%. These data provide a smooth theoretical reference for line identification.

Also presented is a systematic second-order relativistic MBPT study of reduced matrix elements and oscillator strengths for dipole transitions into the ground state in Ni-like ions, with nuclear charges ranging from $Z=29$ to 100. The retarded dipole matrix elements include correlation corrections from Coulomb and Breit interactions. Both length and velocity forms of the matrix elements were evaluated, and small differences, caused by the nonlocality of the starting HF potential, were found between the two forms. Second-order MBPT transition energies were used to evaluate oscillator strengths. The importance of autoionizing states for calculations of the oscillator strengths in low-Z Ni ions was found and discussed. We believe that our results will be useful in analyzing existing experimental data and in planning new experiments.

ACKNOWLEDGMENTS

The work of W.R.J. was supported in part by National Science Foundation Grant No. PHY-99-70666. U.I.S. acknowledges partial support by Grant No. B503968 from Lawrence Livermore National Laboratory. The work of J.R.A. was performed under the auspices of the U.S. Department of Energy by the University of California, Lawrence Livermore National Laboratory under Contract No. W-7405-Eng-48.

[1] E. Avgoustoglou, W. R. Johnson, D. R. Plante, J. Sapirstein, S. Sheinerman, and S. A. Blundell, Phys. Rev. A **46**, 5478 (1992).
[2] E. Avgoustoglou, W. R. Johnson, Z. W. Liu, and J. Sapirstein, Phys. Rev. A **51**, 1196 (1995).
[3] E. Avgoustoglou and Z. W. Liu, Phys. Rev. A **54**, 1351 (1996).
[4] E. N. Avgoustoglou and D. R. Beck, Phys. Rev. A **57**, 4286 (1998).
[5] J. H. Scofield and B. J. MacGowan, Phys. Scr. **46**, 361 (1992).
[6] M. H. Chen and A. L. Osterheld, Phys. Rev. A **52**, 3790 (1995).
[7] Y. Li, J. Nilsen, J. Dunn, A. L. Osterheld, A. Ryabtsev, and S. Churilov, Phys. Rev. A **58**, R2668 (1998).
[8] H. Daido, S. Ninomiya, M. Takagi, Y. Kato, and F. Koike, J. Opt. Soc. Am. B **16**, 296 (1999).
[9] J. Nilsen, J. Dunn, A. L. Osterheld, and Y. Li, Phys. Rev. A **60**, R2677 (1999).
[10] R. Doron, M. Fraenkel, P. Mandelbaum, A. Zigler, and J. J. Schwob, Phys. Scr. **58**, 19 (1998).
[11] A. Zigler, P. Mandelbaum, J. J. Schwob, and D. Mitnik, Phys. Scr. **50**, 61 (1994).
[12] M. Busquet, D. Pain, J. Bauche, and E. Luc-Koenig, Phys. Scr. **31**, 137 (1985).
[13] M. Klapisch, J. J. Schwob, M. Fraenkel, and J. Oreg, J. Opt. Soc. Am. **61**, 148 (1977).
[14] P. Quinet and E. Biémont, Phys. Scr. **43**, 150 (1991), and references therein.
[15] S. S. Churilov, A. N. Ryabtsev, and J.-F. Wyart, Phys. Scr. **38**, 326 (1988).
[16] J.-F. Wyart, Phys. Scr. **36**, 234 (1987).
[17] M. S. Safronova, W. R. Johnson, and U. I. Safronova, Phys. Rev. A **53**, 4036 (1996).
[18] U. I. Safronova, W. R. Johnson, M. S. Safronova, and A. Derevianko, Phys. Scr. **59**, 286 (1999).
[19] M. H. Chen, K. T. Cheng, and W. R. Johnson, Phys. Rev. A **47**, 3692 (1993).
[20] W. R. Johnson, S. A. Blundell, and J. Sapirstein, Phys. Rev. A **37**, 2764 (1988).
[21] L. W. Fullerton and G. A. Rinker, Jr., Phys. Rev. A **13**, 1283 (1976).
[22] P. J. Mohr, Ann. Phys. (N.Y.) **88**, 26 (1974); **88**, 52 (1974); Phys. Rev. Lett. **34**, 1050 (1975).
[23] W. R. Johnson, D. R. Plante, and J. Sapirstein, Adv. At., Mol., Opt. Phys. **35**, 255 (1995).